

# Bonding in Zintl phase hydrides: Density functional calculations for SrAlSiH, SrAl<sub>2</sub>H<sub>2</sub>, SrGa<sub>2</sub>H<sub>2</sub>, and BaGa<sub>2</sub>H<sub>2</sub>

Alaska Subedi

*Department of Physics and Astronomy, University of Tennessee, Knoxville, Tennessee 37996-1200, USA  
and Materials Science and Technology Division, Oak Ridge National Laboratory, Oak Ridge, Tennessee 37831-6114, USA*

David J. Singh

*Materials Science and Technology Division, Oak Ridge National Laboratory, Oak Ridge, Tennessee 37831-6114, USA*

(Received 15 May 2008; revised manuscript received 9 June 2008; published 9 July 2008)

We investigate the bonding characteristics of SrAlSiH, SrAl<sub>2</sub>H<sub>2</sub>, SrGa<sub>2</sub>H<sub>2</sub>, and BaGa<sub>2</sub>H<sub>2</sub> using density functional calculations. The mixed bonding characteristic of other families of Zintl phases is found, with the formation of covalent  $sp^2$  bonds in the Al/Ga/Al-Si planes of the various compounds. On the other hand the Sr and Ba atoms occur as divalent cations, while the H is anionic. The results indicate that insulating SrSiAlH may be a switchable ferroelectric.

DOI: 10.1103/PhysRevB.78.045106

PACS number(s): 71.20.Ps, 77.84.Bw, 63.20.dk

## I. INTRODUCTION

The electronic and chemical behavior of hydrogen in the solid state has been extensively studied and remains a very active area of research. This is due to fundamental interest in hydrogen chemistry and because of its technological importance, e.g., in passivating semiconductor defects, in metallurgy and in various niche applications such as hydrogen storage. In fact the chemistry of H is perhaps richer than that of any other element with the exception of C. Remarkably, this richness is related to the simplicity of the H atom itself, which consists of a single valence electron and no core electrons.<sup>1</sup> The absence of a core allows very short bond lengths between H and other elements. The one-electron nature of H also leads to a great deal of chemical flexibility with ionization energy and electron affinity compatible with charge transfer in either direction depending on the chemical environment. This underlies the amphoteric behavior of H in many semiconductors leading to its importance in passivating defects. In addition to behaving as a cation or an anion, H can participate in covalent and metallic bonding and also in so-called H bonding. However, even in ionic situations, H is unlike other elements. For example, while the structures of many anionic hydrides have parallels in F chemistry,<sup>2,3</sup> H<sup>-</sup> is a much more flexible ion than F<sup>-</sup>, e.g., in the range of bond lengths that it can take.<sup>4,5</sup>

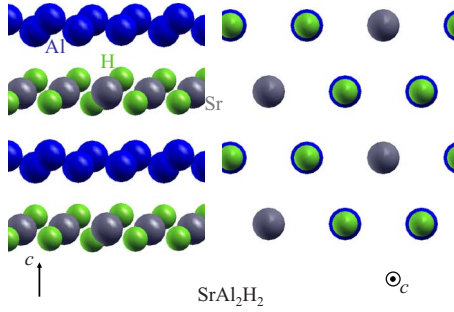
Thus the discovery of the first Zintl phase hydride, SrAl<sub>2</sub>H<sub>2</sub>, by Gintl and coworkers<sup>6</sup> attracted significant interest. This was followed by the discovery of additional members of this family: SrGa<sub>2</sub>H<sub>2</sub>, BaGa<sub>2</sub>H<sub>2</sub>, and SrSiAlH, as well as first-principles studies of the electronic structures of these compounds.<sup>7,8</sup> SrSiAlH is semiconducting in contrast to the other members of the family, which are metallic. The purpose of this paper is to better elucidate the bonding of these compounds, and especially the role of hydrogen, based on density functional calculations. We find that the bonding has mixed character, which is characteristic of other Zintl-type compounds. In particular that Ba and Sr are cationic while H is anionic, and that these ions provide charge balance to support covalent  $sp^2$  bonds among the Al, Ga, and Si atoms.

## II. METHOD

The main results reported here are based on calculations of electronic structures and phonon frequencies in the various compounds and comparisons with model hypothetical compounds to elucidate the bonding. All the calculations were performed within density functional theory with the generalized gradient approximation (GGA) of Perdew, Burke, and Ernzerhof (PBE).<sup>9</sup> The electronic structures and related quantities were obtained using the general potential linearized augmented plane-wave (LAPW) method<sup>10</sup> as implemented in the WIEN2K code.<sup>11</sup> This is an all-electron method that uses a flexible basis and makes no shape approximations to the potential and charge density. Significantly for the present study, the LAPW method uses a partitioning of space into atom centered spheres and an interstitial region, which as will be discussed facilitates analysis of bonding by providing a way of assigning the H contributions. Well-converged basis sets were used with LAPW sphere radii of 2.2, 2.3, 2.1, 2.1, 2.15, and 1.0 $a_0$  for Sr, Ba, Al, Si, Ga, and H, respectively. The phonon dispersions were computed using linear response<sup>12</sup> as implemented in the QUANTUM-ESPRESSO package.<sup>13</sup> We used GGA ultrasoft pseudopotentials<sup>14</sup> with an energy cutoff of 40 Ry. Special attention was paid to the convergence of the grid that represents the charge density as is important when using ultrasoft pseudopotentials in phonon calculations. A (6,6,6) grid was used for the Brillouin zone sampling. The atomic positions were separately relaxed at the experimental lattice parameters for use in calculation of phonon dispersions. There were no significant differences in relaxed positions obtained from the LAPW and pseudopotential calculations.

## III. STRUCTURE

SrAl<sub>2</sub>H<sub>2</sub>, BaGa<sub>2</sub>H<sub>2</sub>, and SrGa<sub>2</sub>H<sub>2</sub> occur in a hexagonal structure, space group  $P\bar{3}m1$ , as shown in Fig. 1. The structure consists of triangular lattice sheets of Sr atoms and dimpled hexagonal sheets of Al atoms. H atoms occur close to the Sr plane in a dimpled hexagonal sheet so that alternat-

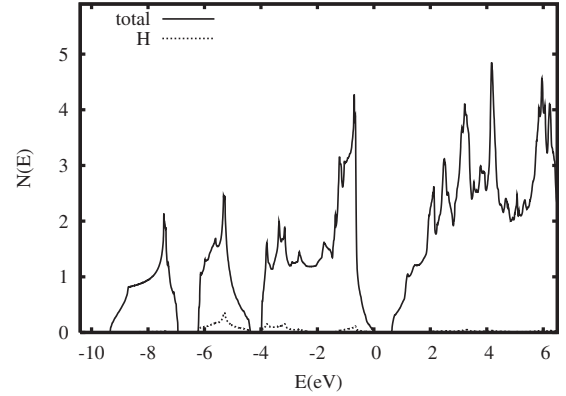
FIG. 1. (Color online) The crystal structure of  $\text{SrAl}_2\text{H}_2$ .

ing H atoms are closer to the Al either above or below the Sr plane, with the corresponding Al atom moving toward its nearest H. This leads to the formation of alternating short and long Al-H distances along the  $c$  axis. This structure is closely related to the structure of intermetallic hydride  $\text{ZrBe}_2\text{H}_x$ , although as will be shown below the bonding is very different from the metallic bonding based on strong hybridization of Zr and Be states found in that material.<sup>15–18</sup> The structure of  $\text{SrAlSiH}$  is similar to that of  $\text{SrAl}_2\text{H}_2$  with the replacement of every other Al atom by Si, and removal of the H atom that was closest to the replaced Al, yielding a noncentrosymmetric  $P3m1$  space group.

The structures used in the present calculations are given in Table I. The atomic positions were relaxed at the experimental lattice parameters, except as noted. These structures agree with prior determinations.<sup>6–8</sup> For example, the experimentally determined nearest-neighbor Al-H distances in  $\text{SrAl}_2\text{H}_2$  and  $\text{SrAlSiH}$  are 1.71 and 1.77 Å, respectively,<sup>6,7</sup> while the calculated values are 1.72 and 1.76 Å, respectively. It is noteworthy that the Al-H and Ga-H distances in these compounds range from 1.702 Å in  $\text{BaGa}_2\text{H}_2$  to 1.761 Å in  $\text{SrAlSiH}$ . These distances are substantially longer than the sums of the covalent radii, which are 1.55 Å, for Al-H, and 1.63 Å, for Ga-H, and furthermore that the trend in the bond length between Al and Ga is opposite to the trend in the covalent radii of Al and Ga.<sup>19</sup>

#### IV. ELECTRONIC STRUCTURE OF $\text{SrAlSiH}$

We start our discussion with  $\text{SrAlSiH}$ . The electronic density of states (DOS) of this material is shown in Fig. 2, along

FIG. 2. Electronic density of states of  $\text{SrAlSiH}$  and projection onto the H LAPW sphere.

with the projection onto the H LAPW sphere. The corresponding band structure is shown in the left panel of Fig. 3. We find a band structure similar to that reported previously, and in particular there is a modest semiconducting gap in agreement with prior results.<sup>7,20</sup> The lowest band shown, centered at  $-8$  eV with respect to the valence-band maximum, is of mixed Si  $s$  and Al  $s$  character. The next band, which extends from  $\sim -6$  eV to  $\sim -4$  eV is H  $s$  derived and accounts for the great majority of the H  $s$  character seen in the valence bands. The three remaining occupied bands, extending up to the valence-band edge, are two bands of mixed Si  $p$  and Al  $p$  character, and one band of mainly Si  $p_z$  character ( $p_z$  is the  $p$  orbital directed along the  $c$  axis, while  $p_x$  and  $p_y$  are the  $p$  orbitals directed in the Si-Al plane). The conduction bands have mixed character of mainly Al  $s$ , and Al and Si  $p$  character. As may be seen, the character within the H LAPW sphere is almost entirely located below the Fermi energy, and in particular there is practically no H  $s$  character to the DOS above  $E_F$ . The nominal occupied band electron counting is then two H  $s$  electrons filling the H  $s$  orbital, two Al/Si  $s$  electrons for average half filling of the Al/Si  $s$  orbitals, four Al/Si  $p_x/p_y$  electrons for half filling of those orbitals, and two Si  $p_z$  electrons filling that shell. This electronic structure is then consistent with a view in which there are covalent bonds between Al and Si, in particular  $\sigma$

TABLE I. Structures of  $ABB'X_n$ ,  $A=\text{Sr}, \text{Ba}$ ,  $B=\text{Al}, \text{Ga}$ ,  $B'=\text{Al}, \text{Ga}, \text{Si}$ ,  $X=\text{F}, \text{H}$ , and  $n=0$  for  $\text{KAlSi}$  and  $\text{SrAlSi}$ ,  $n=1$  for other  $B'=\text{Si}$  compounds, and  $n=2$  for  $B=B'=\text{Al}, \text{Ga}$ . The internal coordinates are from GGA structure relaxation, except for  $\text{KAlSi}$ , while the lattice parameters are from experimental data.  $d_{B-X}$  denotes the distance between the  $B$  and  $X$  atoms, e.g., the shortest Al-H bond length in  $\text{SrAl}_2\text{H}_2$ .  $h$  is used to denote hypothetical compounds.

	$a$ (Å)	$c$ (Å)	$z_B$	$z_{B'}$	$z_X$	$d_{B-X}$ (Å)
$\text{SrAl}_2\text{H}_2$	4.528	4.722	0.4608		0.0964	1.721
$\text{SrGa}_2\text{H}_2$	4.401	4.711	0.4646		0.1026	1.705
$\text{BaGa}_2\text{H}_2$	4.533	4.907	0.4694		0.1226	1.702
$\text{SrAlSiH}$	4.214	4.955	0.5403	0.4454	0.8956	1.761
$\text{KAlSi}$ ( $h$ )	4.214	4.955	0.5403	0.4454		
$\text{SrAlSiF}$ ( $h$ )	4.214	4.955	0.5225	0.4401	0.9040	1.891
$\text{SrAlSi}$	4.215	4.770	0.4994	0.5005		

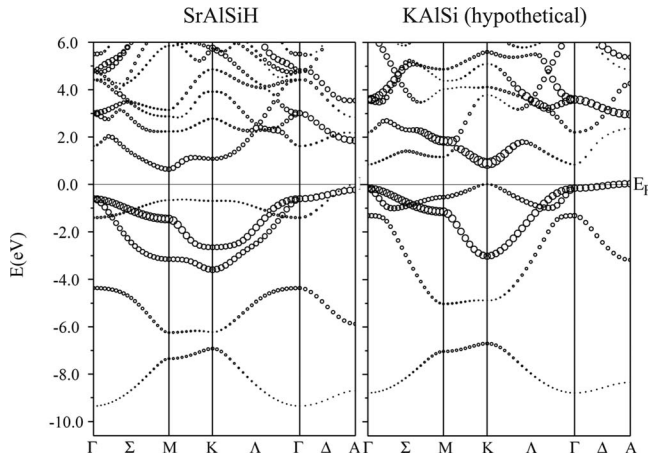


FIG. 3. Electronic band structures of SrAlSiH (left) and hypothetical KAlSi (right), plotted with circles of size proportional to the Al  $p$  character, as defined by projection onto the Al LAPW sphere.

bonding of  $sp^2$  hybrids, while the Sr is close to a  $Sr^{2+}$  cation, as might be expected, and H occurs as the  $H^-$  anion. In addition, the electronic structure is consistent with the existence of weaker Si  $p_z$ -Al  $p_z$   $\pi$  bonding, but the present results are not sufficient for analyzing this in detail. In this picture there are not substantial covalent bonds between Al and H.

In order to better define this picture in relation to an alternate scenario with largely covalent Al-H interactions, we begin with projected density of states. Qualitatively, the feature of having little H  $s$  character above the Fermi energy is similar to what is found in model compounds with anionic H, in particular tetragonal  $MgH_2$  (Ref. 21) and face-centered-cubic  $LiH$ .<sup>22,23</sup> This is in contrast to more covalent systems where antibonding states with significant H character can generally be found in the unoccupied spectrum. In hydrogen anion based materials, the  $H^-$  ion is stabilized by the Ewald field. Thus we consider an ionic model, based on the charge density of a  $H^-$  ion stabilized by the Ewald field, as simulated by a Watson sphere of radius  $2.0a_0$ .<sup>24</sup> For such a  $H^-$  ion in the local density approximation, the charge inside the muffin-tin radius of  $1.0a_0$  is  $0.482e$ . Dividing the integrated DOS of H below the Fermi energy (0.460) by  $0.482e/2$  gives  $1.910e$ . Thus, we can infer that H acquires an electron to fill its  $1s$  orbital.

It is helpful to compare the band structure of SrAlSiH (Fig. 3) in relation to real and hypothetical model compounds in order to gain further insight into the bonding. First we consider SrAlSi, whose band structure is shown in Fig. 4. This band structure is qualitatively very similar to that of SrAlSiH (Fig. 3) except for the missing H  $s$  derived band and an upward shift of the Fermi energy by one electron in the nonhydrogen containing compound, and is close to that obtained previously.<sup>25-27</sup> This implies that the bonding nature of Al and Si in SrAlSiH and SrAlSi is similar and the presence of H in SrAlSiH has little effect on the bonding of Al and Si. Instead H behaves as an anion whose removal thus electron dopes the band structure. Next we consider the band structure of hypothetical KAlSi, which is shown in Fig. 3. This band structure was obtained at the same lattice param-

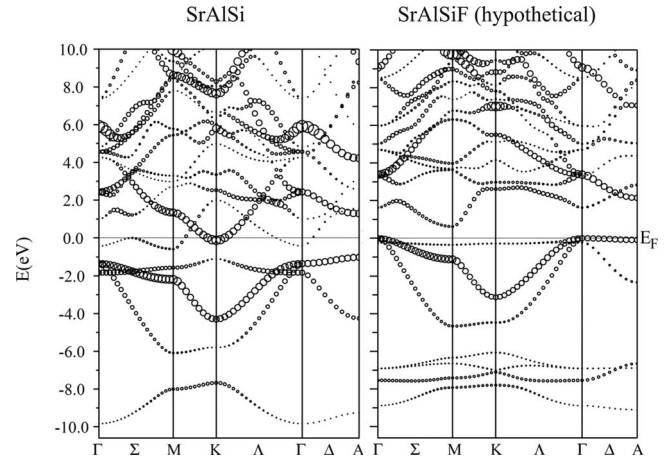


FIG. 4. Electronic band structures of SrAlSi (left) and hypothetical SrAlSiF (right) plotted with symbols of size proportional to the Al  $p$  orbital character (plus a very small size to show the position of bands with no Al  $p$  character).

eters as SrAlSiH with the K placed in the Sr site, followed by relaxation of the internal coordinates. This relaxation yields very small shifts of the atomic positions relative to those of SrAlSiH. Again the band structure is similar to SrAlSiH except for the missing H  $s$  band. The main difference is a lowering in energy and increase in dispersion of the Si  $p_z$  derived bands. The greater sensitivity of the Si  $p_z$  orbital to the details of the Sr-H plane is as would be expected considering that this orbital is directed toward that plane. Like SrAlSi, KAlSi has only four bands below the Fermi energy between 0 and  $-10.0$  eV. These mixed  $s$  and  $p$  bands of Al and Si will be discussed later when we describe the bonding between Al and Si. The fact that, excepting the H  $s$  band, the band structure of SrAlSiH can be reasonably reproduced with the Sr-H layer replaced by monovalent K is a strong indication that the H is at best weakly covalent with Al and that its main role is in accepting charge.

Finally, we consider the band structure of hypothetical SrAlSiF, which is shown in Fig. 4. As mentioned, in many cases there are close analogies between compounds based on  $H^-$  and fluorides. This calculation was done similarly to that of hypothetical KAlSi, with fixed lattice parameters and relaxed internal coordinates. Again we find a band structure rather similar to that of SrAlSiH, with the exception that the H  $s$  band is removed and three additional bands derived from the three occupied  $p$  orbitals of  $F^-$  occur in the valence bands. These three F  $p$  bands occur between  $-6$  and  $-8$  eV. Like SrAlSiH, hypothetical SrAlSiF is a semiconductor, which is perhaps not surprising if one considers that the fluoride anion is replacing a hydride anion of the same charge. The main difference in the occupied Sr-Al derived bands is a small upward shift and decrease in the dispersion of the Si  $p_z$  derived band, which as noted above is expected to be particularly sensitive to the details of the Sr-H layer. Since the three bands showing F  $p$  character all lie below the Fermi energy, F obtains one electron from Sr to get its  $p$  orbital filled. This is not surprising considering the high electronegativity of F. The Pauling electronegativity of H is also higher than Al and Si. This suggests that normally charge



transfer onto Al-H units would preferentially go to H rather than Al. The similarities between SrAlSiH, KAlSi, and SrAlSiF therefore support the view that H obtains one electron to fill its  $s$  orbital and is anionic.

We now return to the bonding between Al and Si in SrAlSiH. As mentioned above, the  $s$  character of both Al and Si is prominent in the lowest band that occurs between  $-6.0$  and  $-8.0$  eV. The Si  $p$  character is pronounced in the three bands below the Fermi energy that lie between  $0.0$  and  $-4.0$  eV. However, Al  $p$  character is conspicuous in only two of these bands that dip below  $-2.0$  eV. Let us remind ourselves that the Al-Si layer has a hexagonal structure. We have also shown that only  $s$ ,  $p_x$ , and  $p_y$  orbitals of Al and Si take part in the bonding. This implies that there is a  $\sigma$  bond between hybridized  $sp^2$  orbitals of Al and Si. It is also notable that there is more Si character than Al in each of these three bands, implying a polar  $\sigma$  bond. This is not surprising since Si is more electronegative than Al. The extra electron from Sr is transferred primarily to the Si so that there are two electrons in its  $p_z$  orbital. However, there is little covalent bonding between the Sr-H and Al-Si layers as there is no mixing of H  $s$  with  $s$  and  $p$  orbitals of Al and Si. Hence, SrAlSiH is perhaps better described as having mixed bonding character as in other Zintl-type phases rather than as a polyanionic compound.

The band structure of SrAlSi (Fig. 4) also has four bands between  $0.0$  and  $-10.0$  eV that are similar to the bands of SrAlSiH (Fig. 3). These bands have Al and Si  $s$  and  $p$  characters. The lowest band lies between  $-7.0$  and  $-10.0$  eV and has mixed Al  $s$  and Si  $s$  character. The three bands just below the Fermi energy have Si  $p$  character, which is mixed with Al  $p$  character for two of them. This again suggests that there is  $\sigma$  bonding between hybridized  $sp^2$  orbitals of Al and Si, and Si obtains one electron from Sr so that there are two electrons in its  $p_z$  orbital, which then is the origin of the third band.

The band structure of SrAlSiF (Fig. 4) has seven bands between  $0.0$  and  $-10.0$  eV. However, except for the three bands between  $-6.0$  and  $-8.0$  eV that show F  $p$  character, this band structure is remarkably similar to those of KAlSi and SrAlSi. The lowest band still shows Al and Si  $s$  character. Two of the first three bands below the Fermi energy again have mixed Al and Si  $p$  character. The third band shows very dominant Si  $p$  character from the  $p_z$  orbital. Thus the Al and Si layer in SrAlSiF are bonded by  $\sigma$  bonds between hybridized  $sp^2$  orbitals. The substitution of H by F in SrAlSiH does not seem to change the bonding behavior of Al and Si in these compounds. Therefore, we can now conclude that H does not play a substantial role in the bonding of Al and Si other than providing for charge balance.

Figure 5 shows the valence charge density for SrAlSiH. As may be seen there is a noticeable bond charge between Al and Si with a maximum in the valence charge density between the atoms. This feature is absent between Al and H but rather there is a buildup of charge centered at the H site. One may note that the Al-H bond lengths in SrAlSiH and SrAl<sub>2</sub>H<sub>2</sub> (see below) are similar to those in NaAlH<sub>4</sub> and Li<sub>3</sub>AlH<sub>6</sub>. The electronic structure of NaAlH<sub>4</sub> was studied in detail by Ozolins and coworkers<sup>28</sup> who described the compound as polar covalent and also as having a highly ionic nature, and by

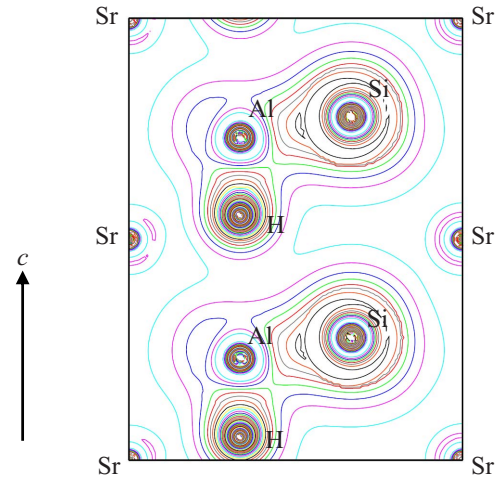


FIG. 5. (Color online) Valence charge density (not including semicore states) for SrAlSiH in a plane passing through the atoms. The contours are in equally spaced increments of  $0.05e/\text{\AA}^3$  and start at  $0.05e/\text{\AA}^3$ . Note the bond charge between Si and Al, but not between Al and H, and also the buildup of valence charge around H and Si.

Aguayo and coworkers who made arguments that the compound is largely ionic.<sup>29</sup> A more detailed analysis was applied to Li<sub>3</sub>AlH<sub>6</sub> also finding substantial ionic character in that case.<sup>30</sup> Those results are consistent with what is found here for the Al-H interaction. Thus the Zintl hydride SrAlSiH differs from complex hydrides, such as NaAlH<sub>4</sub> mainly in having a covalently bonded Si-Al backbone, which may offer different possibilities for chemical tuning of the properties.

## V. SrAl<sub>2</sub>H<sub>2</sub>

We now discuss the bonding of SrAl<sub>2</sub>H<sub>2</sub>. Our density of states and band structure are similar to that obtained previously by Orgaz and Aburto.<sup>31</sup> As mentioned earlier, this material is very similar to SrAlSiH. The Si is replaced by Al and H, so we now have Al-Al and Sr-H<sub>2</sub> layers instead of Al-Si and Sr-H ones. The electronic density of states of SrAl<sub>2</sub>H<sub>2</sub> is shown in Fig. 6. Almost all of the H character occurs below

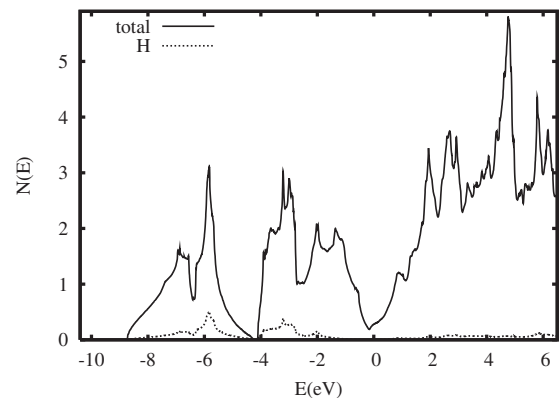


FIG. 6. Electronic density of states of SrAl<sub>2</sub>H<sub>2</sub> and projection onto the H LAPW sphere.

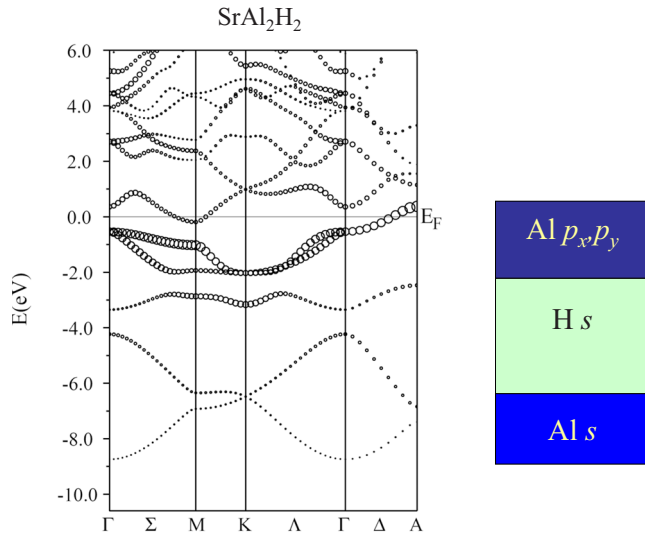


FIG. 7. (Color online) Electronic band structure of  $\text{SrAl}_2\text{H}_2$  (right) plotted with symbols of size proportional to the Al  $p$  orbital character (plus a very small size to show the position of bands with no Al  $p$  character). The left panel is a schematic showing the regions in the valence bands where various orbital characters are dominant.

Fermi energy indicating that H atoms are anionic. Again, we consider the ionic model where the  $\text{H}^-$  ion is stabilized by the Ewald field. As mentioned above, the charge inside the radius of  $1.0a_0$  is  $0.482e$ . The integrated DOS of H below the Fermi energy is 0.897. Dividing this number by  $0.482e/2$  and recalling that there are two H per cell one obtains  $1.86e/\text{H}$ , i.e., very close to  $\text{H}^-$ .

We can gain more insight about the bonding in  $\text{SrAl}_2\text{H}_2$  by studying its band structure, which is shown in Fig. 7. Near the Fermi energy, there are two bands of Al  $p$  character that stay mostly below the Fermi level, but cross along  $\Gamma$ -A, leading to semimetallic character. In particular these two bands lead to hole Fermi surfaces around A, which are compensated by an electron pocket around M.

The next lower two bands that lie between  $-2.0$  and  $-7.0$  eV have H  $s$  character, confirming that  $s$  orbitals of two H atoms are filled. Finally, Al  $s$  character is prominent in the fifth band below the Fermi level which reaches a high of approximately  $-6.5$  eV at the K point and a low of approximately  $-9.0$  eV at  $\Gamma$ . As in  $\text{SrAlSiH}$ , there is little H  $s$  character in the conduction bands. As mentioned earlier, the Al-Al layer has a hexagonal structure. This suggests that the  $s$ ,  $p_x$ , and  $p_y$  orbitals of Al hybridize into  $sp^2$  orbitals and each Al atom is  $\sigma$  bonded with three other Al atoms. Within this scenario the main difference between semiconducting  $\text{SrAlSiH}$  and metallic  $\text{SrAl}_2\text{H}_2$  is that in the silicide the  $p_z$  orbital of Si is occupied, and the  $sp^2$   $\sigma$  bonds take some polar character, this latter feature leading to the semiconducting gap. In both compounds the role of Sr and H is to provide charge balance. In particular, we note that in  $\text{SrAl}_2\text{H}_2$  the Al layers are nominally neutral (i.e., not polyanionic).

## VI. PHONON DISPERSIONS AND GALLIUM COMPOUNDS

Phonon dispersions are often useful in understanding bonding. Generally speaking, a covalent H bond is stronger

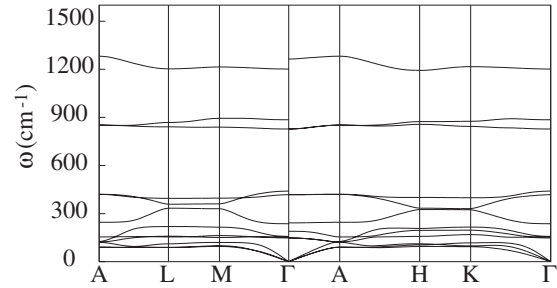


FIG. 8. Calculated phonon dispersion curves along several high-symmetry directions for  $\text{SrAlSiH}$ .

than an anionic H bond, and has both a shorter bond length and higher force constants. For comparison, experimental vibrational frequencies of symmetric stretching modes of the covalently bonded  $\text{NH}_3$  and  $\text{H}_2\text{O}$  molecules are  $3336$  and  $3657$   $\text{cm}^{-1}$ , respectively (Ref. 32). On the other hand, the largest vibrational frequencies of fcc LiH and tetragonal  $\text{MgH}_2$  obtained from the calculated phonon dispersion curves are around  $1100$  and  $1500$   $\text{cm}^{-1}$ , respectively.<sup>33,34</sup> The phonon dispersion curves of  $\text{SrAlSiH}$  and  $\text{SrAl}_2\text{H}_2$  are shown in Figs. 8 and 9, respectively. From these plots, the largest phonon frequencies for  $\text{SrAlSiH}$  and  $\text{SrAl}_2\text{H}_2$  are approximately  $1280$  and  $1430$   $\text{cm}^{-1}$ , respectively. For comparison, the bond stretching frequency of the GaH dimer is  $1605$   $\text{cm}^{-1}$  and that of AlH is  $1670$   $\text{cm}^{-1}$ . We note that these maximum frequencies are close to the maximum frequencies reported in the calculations of Ref. 20, but that our dispersions have some minor but possibly significant quantitative differences, especially nonanalytic character at  $\Gamma$  for SrAlSiH, as would be anticipated for an ionic insulator. The differences between our calculation and that of Lee and co-workers are, however, too small to distinguish based on existing neutron-scattering data.<sup>20</sup>

Our results for the electronic structure and phonon dispersions of the gallium compounds,  $\text{SrGa}_2\text{H}_2$  and  $\text{BaGa}_2\text{H}_2$ , are given in Figs. 10–12. As may be seen, the electronic structures have strong similarities to those of the  $\text{SrAl}_2\text{H}_2$  in the valence region and that the phonon dispersions are also similar to those of the Al based compound with the exception that the metal derived phonon frequencies of the gallium compounds are lower due to the heavier mass of Ga relative to Al. As for the Al compounds, the H derived phonon bands consist of two narrow bands—a longitudinal band at the highest frequencies and a transverse band with twice as

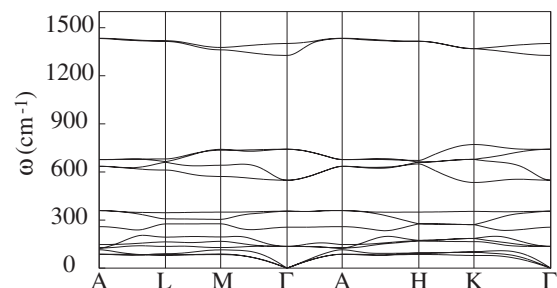


FIG. 9. Calculated phonon dispersion curves along several high-symmetry directions for  $\text{SrAl}_2\text{H}_2$ .

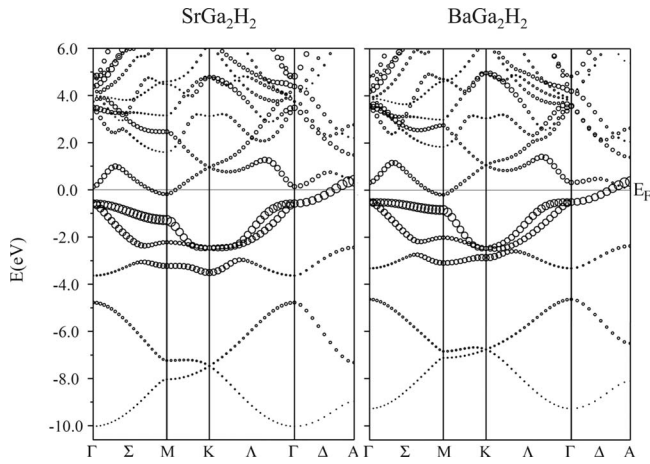


FIG. 10. Electronic band structures of  $\text{SrGa}_2\text{H}_2$  (left) and  $\text{BaGa}_2\text{H}_2$  (right) plotted with symbols of size proportional to the Ga  $p$  orbital character (plus a very small size to show the position of bands with no Ga  $p$  character).

many modes at lower frequency. Both of these bands are well above the highest metal atom derived phonon band in these materials. This separation into narrow well-separated phonon bands is characteristic of materials with large mass differences between the atoms and relatively weak bonding. In any case, the bonding of the gallium compounds can therefore be analyzed in a similar way to that of  $\text{SrAl}_2\text{H}_2$  with the conclusion that the Ga layers are  $sp^2$   $\sigma$  bonded and that H occurs as the  $\text{H}^-$  anion.

## VII. DISCUSSION AND CONCLUSIONS

We report a series of electronic structure calculations for the Zintl phase hydrides and model compounds. Comparison of the electronic structures leads to the conclusion that in these phases the Al/Si/Ga layers are stabilized by  $sp^2$  covalent bonding, and that the Sr and H atoms occur as ions that provide charge balance. Within this framework the semiconducting nature of  $\text{SrAlSiH}$  is due to polarization of the Al-Si bond. We note that the concept of electronegativity is an important one in chemistry, and especially solid-state chemistry where the long-range Ewald potential favors larger charge transfers than in molecules. The present conclusion that these phases are based on the hydride anion is consistent with the high electronegativity of H relative to Al and Ga.

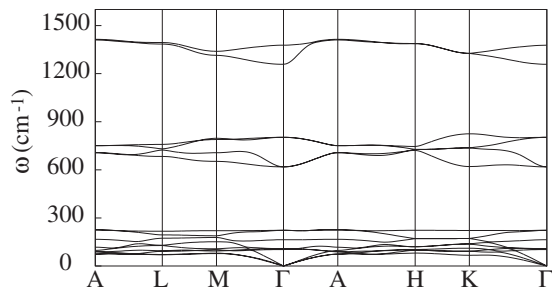


FIG. 11. Calculated phonon dispersion curves along several high-symmetry directions for  $\text{SrGa}_2\text{H}_2$ .

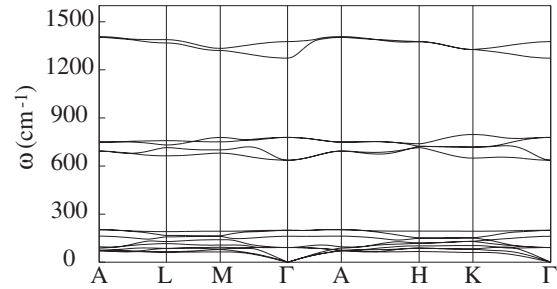


FIG. 12. Calculated phonon dispersion curves along several high-symmetry directions for  $\text{BaGa}_2\text{H}_2$ .

Characterizing the nature of bonds in solids in terms of charge transfer involves ambiguity since there is no unique way of partitioning space into regions that can be associated with the atoms and because expansions around atomic sites become overcomplete as basis functions are added. However, such characterizations are often very useful in understanding the properties of compounds, the relationships between different compounds, and in finding new related phases. We hope that the present characterization of the bonding in the Zintl phase hydrides will be useful in identifying new members of this family and better understanding their chemical and physical properties.

We find that  $\text{SrAlSiH}$  is stabilized by ionic bonds and occurs in a noncentrosymmetric polar structure. This structure is generated from an ideal nonpolar structure with  $z_{\text{H}}=0.0$  and  $z_{\text{Al}}=z_{\text{Si}}=0.5$  by displacements of H and Al in opposite directions by  $\sim 0.5$  Å in the case of H and  $\sim 0.2$  Å for Al, accompanied by a displacement of Si by  $\sim 0.25$  Å in the same direction as H. Considering that in our picture of the bonding Si and H take the charge provided by Sr, this is a structure in which the anions (H and Si) move opposite to the Al and Sr. The fact that the displacements are in the several tenths of Angstrom range suggests that the structure may be switchable, as in, e.g.,  $\text{BiFeO}_3$  and  $\text{LiNbO}_3$ . This is an interesting result because while ferroelectrics containing hydrogen are known, they are phases containing complex anions such as hydrogen phosphate. To our knowledge, if  $\text{SrAlSiH}$  is ferroelectric, it would be the first inorganic ferroelectric based on the hydride anion. It would be of interest to perform high electric-field low-temperature measurements on  $\text{SrAlSiH}$  to determine if it can be poled and dielectric measurements to determine if ferroelectric switching and hysteresis loops can be obtained.

In this regard, we calculated the energy of the fully symmetric structure in which, Al, Si and H were all placed on the reflection planes. This is intermediate between the up and down polarized  $\text{SrAlSiH}$  structures, and therefore provides an upper bound on the energy barrier for switching. The calculated energy is 0.27 eV above the relaxed structure consistent with ferroelectric switching.<sup>35</sup> The calculated electronic dielectric constant as obtained from linear response is high reflecting the relatively small gap:  $\epsilon_{xx}=\epsilon_{yy}=13.4$  and  $\epsilon_{zz}=11.3$ . The Born effective charges also obtained from the linear-response calculations without enforcing the acoustic sum rule are  $Z_{xx}^*(\text{Sr})=2.1$ ,  $Z_{zz}^*(\text{Sr})=2.3$ ,  $Z_{xx}^*(\text{Al})=2.2$ ,  $Z_{zz}^*(\text{Al})=1.3$ ,  $Z_{xx}^*(\text{Si})=-2.7$ ,  $Z_{zz}^*(\text{Si})=-2.7$ ,  $Z_{xx}^*(\text{H})=-1.4$ , and



$Z_{zz}^*(\text{H}) = -1.7$ . One may note that the Born charges are enhanced over the nominal values and are anisotropic. Enhancement of Born charges is characteristic of ionic materials with cross-gap hybridization, such as oxide ferroelectrics.<sup>36</sup> In contrast, covalent materials such as GaAs generally have Born effective charges that are reduced from the nominal values.

As mentioned, the Ewald potential, which is important in the stabilization of ionic structures, is long ranged. Therefore, the bonding of such materials is typically quite sensitive to chemical substitutions. While for example, partial substitution in the Sr site might not be expected to be very important in the stabilization of a supposed Al-H covalent bond, they could well have a large effect on the stability of hydride anions in the structure based on the bonding that we find. In addition, ionic bonding can be strongly affected by

dielectric screening. So for example, it may be that chemical modification that improves the metallicity of the semimetallic Al layers in  $\text{SrAl}_2\text{H}_2$  or that metalizes the Al-Si layer in  $\text{SrAlSiH}$  would destabilize the hydride anions in those compounds. Also, it may be that small scale nanostructuring to produce interfaces with metallic compounds including carbons would also destabilize the hydride anions—a result that would not be expected in a covalently bonded system.

#### ACKNOWLEDGMENTS

This work was supported by the Department of Energy, Office of Basic Energy Sciences, Division of Materials Sciences and Engineering (ORNL) and the Office of Naval Research (UT).

- 
- <sup>1</sup>L. Pauling, *The Nature of the Chemical Bond and the Structure of Molecules and Crystals: An Introduction to Modern Structural Chemistry*, 3rd ed. (Cornell University Press, Ithaca, 1960).
- <sup>2</sup>C. E. Messer, *J. Solid State Chem.* **2**, 144 (1970).
- <sup>3</sup>K. Yvon, *Chimia* **52**, 613 (1998).
- <sup>4</sup>D. F. C. Morris and G. L. Reed, *J. Inorg. Nucl. Chem.* **27**, 1715 (1965).
- <sup>5</sup>R. D. Shannon, *Acta Crystallogr., Sect. A: Cryst. Phys., Diffr., Theor. Gen. Crystallogr.* **32**, 751 (1976).
- <sup>6</sup>F. Gingl, T. Vogt, and E. Akiba, *J. Alloys Compd.* **306**, 127 (2000).
- <sup>7</sup>T. Bjorling, D. Noreus, K. Jansson, M. Andersson, E. Leonova, M. Edén, U. Hälenius, and U. Häussermann, *Angew. Chem., Int. Ed.* **44**, 7269 (2005).
- <sup>8</sup>T. Bjorling, D. Noreus, and U. Häussermann, *J. Am. Chem. Soc.* **128**, 817 (2006).
- <sup>9</sup>J. P. Perdew, K. Burke, and M. Ernzerhof, *Phys. Rev. Lett.* **77**, 3865 (1996).
- <sup>10</sup>D. J. Singh and L. Nordstrom, *Planewaves Pseudopotentials and the LAPW Method*, 2nd ed. (Springer, Berlin, 2004).
- <sup>11</sup>P. Blaha, K. Schwarz, G. Madsen, D. Kvasnicka, and J. Luitz (<http://www.wien2k.at>).
- <sup>12</sup>S. Baroni, S. de Gironcoli, A. D. Corso, and P. Giannozzi, *Rev. Mod. Phys.* **73**, 515 (2001).
- <sup>13</sup>S. Baroni *et al.* (<http://www.quantum-espresso.org>).
- <sup>14</sup>D. Vanderbilt (<http://www.physics.rutgers.edu/~dhv/uspp>).
- <sup>15</sup>A. J. Maeland and G. G. Libowitz, *J. Less-Common Met.* **89**, 197 (1983).
- <sup>16</sup>A. J. Maeland, *J. Less-Common Met.* **89**, 173 (1983).
- <sup>17</sup>A. F. Andresen, K. Otnes, and A. J. Maeland, *J. Less-Common Met.* **89**, 201 (1983).
- <sup>18</sup>D. J. Singh and M. Gupta, *Phys. Rev. B* **76**, 075120 (2007).
- <sup>19</sup>Here we use the usual covalent radii of Al, Ga, and H of 1.18 Å, 1.26 Å, and 0.37 Å, based on nonpolar compounds and in particular the  $\text{H}_2$  molecule for H. Generally polar bonds will be shorter, and in fact a value of 0.30 Å for H is often used, e.g., Ref. 1.
- <sup>20</sup>M. H. Lee, O. F. Sankey, T. Bjorling, D. Moser, D. Noreus, S. F. Parker, and U. Häussermann, *Inorg. Chem.* **46**, 6987 (2007).
- <sup>21</sup>R. Yu and P. K. Lam, *Phys. Rev. B* **37**, 8730 (1988).
- <sup>22</sup>A. B. Kunz and D. J. Mickish, *Phys. Rev. B* **11**, 1700 (1975).
- <sup>23</sup>R. Dovesi, C. Ermondi, E. Ferrero, C. Pisani, and C. Roetti, *Phys. Rev. B* **29**, 3591 (1984).
- <sup>24</sup>R. E. Watson, *Phys. Rev.* **111**, 1108 (1958).
- <sup>25</sup>I. I. Mazin and D. A. Papaconstantopoulos, *Phys. Rev. B* **69**, 180512(R) (2004).
- <sup>26</sup>G. Q. Huang, L. F. Chen, M. Liu, and D. Y. Xing, *Phys. Rev. B* **69**, 064509 (2004).
- <sup>27</sup>G. Q. Huang, L. F. Chen, M. Liu, and D. Y. Xing, *Phys. Rev. B* **71**, 172506 (2005).
- <sup>28</sup>V. Ozolins, E. H. Majzoub, and T. J. Udovic, *J. Alloys Compd.* **375**, 1 (2004).
- <sup>29</sup>A. Aguayo and D. J. Singh, *Phys. Rev. B* **69**, 155103 (2004).
- <sup>30</sup>D. J. Singh, *Phys. Rev. B* **71**, 216101 (2005).
- <sup>31</sup>E. Orgaz and A. Aburto, *Int. J. Quantum Chem.* **101**, 783 (2005).
- <sup>32</sup>G. Herzberg, *Molecular Spectra and Molecular Structure III, Electronic Spectra and Electronic Structure of Polyatomic Molecules* (Krieger, Malabar, FL, 1991).
- <sup>33</sup>J. L. Verble, J. L. Warren, and J. L. Yarnell, *Phys. Rev.* **168**, 980 (1968).
- <sup>34</sup>N. Ohba, K. Miwa, T. Noritake, and A. Fukumoto, *Phys. Rev. B* **70**, 035102 (2004).
- <sup>35</sup>Note that 180° switching in ferroelectrics is normally by domain-wall motion, which would be the expected switching mechanism here.
- <sup>36</sup>W. Zhong, R. D. King-Smith, and D. Vanderbilt, *Phys. Rev. Lett.* **72**, 3618 (1994).